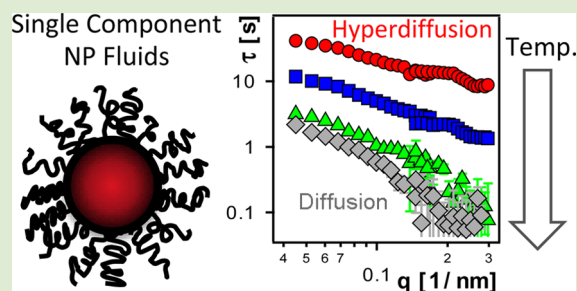


Hyperdiffusive Dynamics in Newtonian Nanoparticle Fluids

Samanvaya Srivastava,^{†,‡} Praveen Agarwal,^{†,‡} Rahul Mangal,[†] Donald L. Koch,[†] Suresh Narayanan,[§] and Lynden A. Archer^{*,†}[†]School of Chemical and Biomolecular Engineering, Cornell University, Ithaca, New York 14853, United States[§]Advanced Photon Source, Argonne National Laboratory, Argonne, Illinois 60439, United States

Supporting Information

ABSTRACT: Hyperdiffusive relaxations in soft glassy materials are typically associated with out-of-equilibrium states, and nonequilibrium physics and aging are often invoked in explaining their origins. Here, we report on hyperdiffusive motion in model soft materials comprised of single-component polymer-tethered nanoparticles, which exhibit a readily accessible Newtonian flow regime. In these materials, polymer-mediated interactions lead to strong nanoparticle correlations, hyperdiffusive relaxations, and unusual variations of properties with temperature. We propose that hyperdiffusive relaxations in such materials can arise naturally from nonequilibrium or non-Brownian volume fluctuations forced by equilibrium thermal rearrangements of the particle pair orientations corresponding to equilibrated shear modes.



Hyperdiffusive relaxations are among the least understood phenomena in soft matter.^{1–13} Typically observed in far-from-equilibrium soft materials, they are thought to reflect a material's response to internal stresses, which are either built in at the glass transition^{6,8} or accrue due to a variety of reasons: for instance, syneresis in attractive colloidal gels,¹ charge accumulation in laponite suspensions,⁴ droplet collapse in emulsions,⁷ or progressive cross-linking of actin filaments.¹¹ Despite their widely dissimilar origins, hyperdiffusive relaxations are characterized by relaxation functions in which the characteristic relaxation time τ varies inversely with the wave vector q , $\tau \sim q^{-1}$. Hyperdiffusive relaxations have also recently been reported in hard sphere glasses,¹⁴ colloidal polycrystals,¹⁵ and metallic glasses,¹⁶ indicating that they are not limited to soft matter. It is also clear from these studies that the length and time scales³ of the relaxation events are much larger than those associated with the ballistic regime in Brownian motion,¹⁷ implying that the forces producing hyperdiffusion must be correlated over long times.

In this Letter, we show that hyperdiffusive relaxations can occur in soft materials that exhibit a readily accessible Newtonian, zero-shear rate viscosity. Fluids comprised of self-suspended nanoparticles created by densely grafting short polymers ($M_w \leq 15000$ Da) to 10 ± 2 nm diameter (d) silica (SiO_2) nanospheres¹⁸ were used for the study. These fluids have been reported previously to behave as model soft glasses owing to their simple, single-component nature and lack of enthalpic interactions.^{19,20} They are therefore good model systems for studying particle interactions and relaxations in nanoparticle/polymer composites comprised of partially²¹ or completely^{22,23} aggregated nanoparticles. Relaxations in these materials were investigated through X-ray photon correlation spectroscopy (XPCS) measurements.¹⁰ Figure 1A reports

representative intermediate scattering functions $g_1(q, t)$ obtained at different wave vectors q from time correlation of the X-ray scattering intensities accessed via XPCS. Samples were maintained in a near vacuum environment at controlled temperature (within ± 0.05 °C) to eliminate any influence of external fluctuations on the measurements.²⁴

$g_1(q, t)$ is the spatial Fourier transform of the time-dependent particle-pair number density correlation function and provides a convenient means of characterizing long-time relaxations. The solid lines in Figure 1A are fits based on a compressed exponential decay of $g_1(q, t)$ with $\tau(q)$ and $\beta(q)$ being q -dependent characteristic relaxation time and compression exponent, respectively, and f being a scaling factor (~ 1) as

$$g_1(q, t) = f \exp \left[\left(-\frac{t}{\tau(q)} \right)^{\beta(q)} \right] \quad (1)$$

Characteristic hyperdiffusive features are evident in the relaxation of our materials, as depicted in Figure 1D,E. The τ - q relationships at multiple q for two representative fluids, 7.3 and 5 kDa polyisoprene (PI) tethered SiO_2 nanoparticles (PI- SiO_2) with particle volume fractions ϕ of 0.033 and 0.054, respectively, clearly exhibit the tell-tale $\tau \sim q^{-1}$ scalings. Similar $\tau \sim q^{-1}$ relationships are reported as Supporting Information (Figure S1) in a large number of soft-glassy systems spanning a range of ϕ . These materials are comprised of PI or polyethylene glycol (PEG) tethered, solvent-free nanoparticle fluids. Hyperdiffusive relaxations are also typically associated with $g_1(q, t)$

Received: May 15, 2015

Accepted: September 18, 2015

Published: September 24, 2015

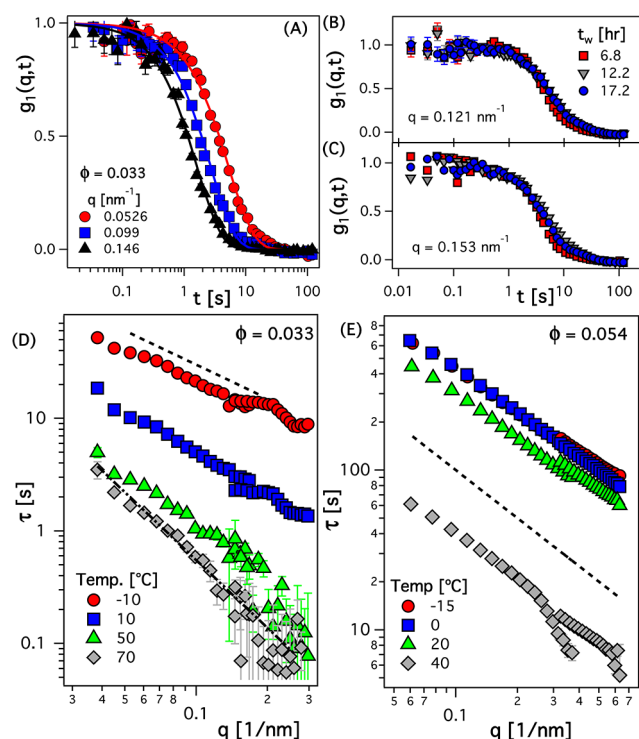


Figure 1. (A) Intermediate scattering functions $g_1(q,t)$ measurement at various q values and 10 °C (symbols) and (B, C) $g_1(q,t)$ at $q = 0.121$ and 0.153 nm^{-1} at different waiting times t_w conducted at 0 °C for 7.3 kDa PI–SiO₂ ($\phi = 0.033$). Solid lines in (A) denote the compressed exponential fits, as shown in eq 1. (D, E) Characteristic relaxation time τ vs wave vector q at different temperatures for 7.3 kDa PI–SiO₂ ($\phi = 0.033$) and 5 kDa PI–SiO₂ ($\phi = 0.054$) nanoparticle fluids, respectively. Dashed and dashed-double dot lines correspond to -1 and -2 power laws, respectively. Error bars are shown only for data sets where they are larger than the symbols. The discontinuity in data sets is a result of two separate measurements in different q ranges.

taking a compressed exponential functional form, with $\beta \sim 1.5$.^{1,3} This behavior is consistent with our observations, as shown in the q -dependence of β for a large number of materials (Figure S2). We considered two forms of eq 1 in the study. In the first approach, β was allowed to vary independently and β values within $1.1 < \beta < 1.9$ were found from best fits of the compressed exponential form to the $g_1(q,t)$ experimental data. β values in this range are consistent with observations for other materials that exhibit hyperdiffusive relaxation.^{8,25–27} In the second approach, a fixed $\beta = 1.5$ was used. Both methods yielded $\tau \sim q^{-1}$, as shown in Figure S3, indicating that the hyperdiffusive nature of the relaxations is independent of the fitting approach.

The range of length scales over which hyperdiffusive relaxations were observed is also noteworthy; the characteristic length scale $l \sim 2\pi/q$ ranges from 10 to 165 nm (approximately 1–16 \times the nanoparticle diameter d), signifying that the XPCS measurements probed particle relaxations at length scales much larger than those associated with the ballistic regime in Brownian motion ($\ll d$). The measurements also spanned the primary peak of the static structure factor, and the typical interparticle separations $\lambda (=d(0.64/\phi)^{1/3} \sim 15\text{--}30 \text{ nm})$ in the materials. Additionally, a transition to diffusive relaxations ($\tau \sim q^{-2}$) was observed in fluids with $\phi = 0.023$ and 0.033 at temperatures higher than 70 °C (Figures 1D). Later in the manuscript, we will argue that this observed transition to

diffusive behavior is important and provides insights about the requirements for hyperdiffusive relaxation.

Hyperdiffusive relaxations are typically associated with non-equilibrium forces, and are usually accompanied by strong aging of the material properties with time. Figure 1B,C shows $g_1(q,t)$ traces obtained at two different q values after various waiting times t_w from the beginning of the experiment. The similarity of the $g_1(q,t)$ traces across time scales more than 3 orders of magnitude larger than τ (e.g., $t_w = 17 \text{ h} \approx 6000\tau$) means that temporal phenomena such as aging are insignificant in these materials and do not contribute to the relaxations observed through XPCS measurements. Similar compressed exponential dynamics with nonaging characteristics have been previously reported for diblock copolymer–homopolymer blends with sponge phases.²⁸

Along with nonaging behavior, self-suspended nanoparticle fluids are also able to relax completely under shear, as is evident from shear flow rheology experiments. The steady shear results, reported in Figure 2, show that nanoparticle fluids with low ϕ

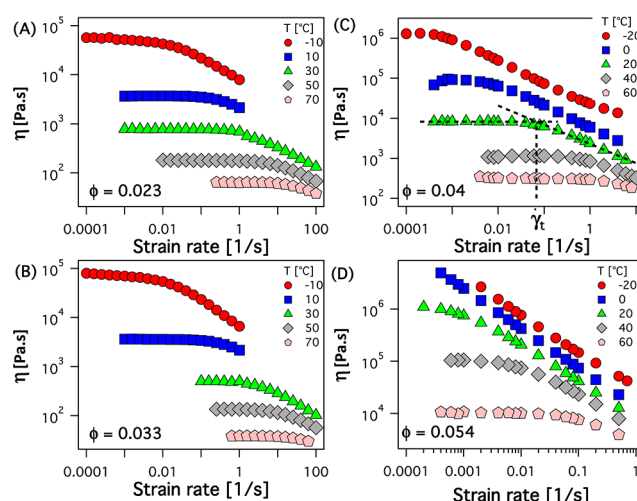


Figure 2. Rate sweeps at different temperatures from rheology measurements for (A) 13.4 kDa PI–SiO₂ ($\phi = 0.023$), (B) 7.3 kDa PI–SiO₂ ($\phi = 0.033$), and (C, D) 5 kDa PI–SiO₂ ($\phi = 0.04$ and $\phi = 0.054$) nanoparticle fluids. In (C), dashed lines denote a representative transition shear rate.

($\phi \leq 0.054$), which exhibit hyperdiffusive relaxations (Figures 1D,E), display flow behavior reminiscent of moderately concentrated suspensions with a readily accessible Newtonian flow regime (characterized by a shear viscosity that is independent of the imposed shear rate, shear strain, and time). At shear rates above a characteristic value $\dot{\gamma}_t$ (see Figure 2C), which varies with temperature and material composition, the Newtonian flow regime gives way to shear thinning rheology, allowing us to define a characteristic shear rheological relaxation time $\tau_r (= 1/\dot{\gamma}_t)$. This time scale is associated with the rate at which shear-induced configurations of the material disappear upon cessation of shearing motion. Additionally, in the Newtonian flow regime, a fluid's viscosity is a material function, implying that the studied materials may be considered at equilibrium over time scales $\geq \tau_r$.

Figures 1 and 2 summarize our main observation: density correlations can decay as compressed exponentials in macroscopically Newtonian materials. A theoretical argument based on the Smoluchowski equation for Brownian suspensions with any arbitrary interparticle potential leads to the constraint

$(-1)^n(\partial^n g_1/\partial t^n) > 0$ for all t , provided that the suspension relaxes to an equilibrium state at long times.²⁹ Since the compressed exponential decay of g_1 observed in our experiments violates this constraint, we surmise that (i) the system is not Brownian, (ii) it does not relax to a true equilibrium state, or both. The non-Brownian nature of our materials could arise from the fact that their fluidity is provided by tethered polymers, which are neither continuum nor Newtonian on the length and time scales of particle motion. Dielectric relaxation experiments in similar self-suspended materials²⁰ reveal large increases in the configurational relaxation time of the polymers upon tethering to nanoparticles. It is thus possible that the relaxation process involves the dynamics of the highly constrained polymers as well as the configuration of the particle cores. Second, it is possible that the volumetric modes of the system that are probed by XPCS measurements, and are constrained by the space filling requirement imposed on the particles and the tethered polymers may not relax to a true equilibrium state, while the shear modes probed by rheological measurements do. Under the latter hypothesis, the Newtonian plateau of the shear viscosity would arise from the relaxation of the shear modes, while the volume modes exist in a metastable state that is not perturbed by the solenoidal bulk deformation produced in shear rheology measurements. This hypothesis, however, would imply that $g_1(q,t)$ should not decay completely to zero. We have not detected a nonzero long time g_1 , but this possibility cannot be completely excluded.

Under either of these hypotheses, the shear modes of the system relax to equilibrium, yielding Newtonian behavior ($\phi \leq 0.054$), while the volume modes are more highly constrained. The hyperdiffusive motion in these Newtonian materials is then postulated to arise from an elastic stress due to volumetric relaxation modes to thermal fluctuations in the orientation of neighboring particle pairs which, through their interaction, exert force dipoles on the surrounding material. A strong elastic stress response to volume deformations is expected in self-suspended nanoparticle fluids because the tethered fluid is required to uniformly fill the interparticle space.^{19,20,30,31} To make these inferences concrete, we write down a simple conservation equation for the elastic volumetric deformation u at a point \mathbf{r} produced by a force dipole of strength \mathbf{P}_0 created by a volume deformation located at \mathbf{r}_0 :³²

$$6\pi\eta n \frac{\partial u}{\partial t} - K\nabla^2 u = \mathbf{P}_0 \cdot \nabla \delta(\mathbf{r} - \mathbf{r}_0) \quad (2)$$

Here, K , η , n , and a are bulk modulus, local viscosity, particle number density, and particle radius, respectively. The strain field propagates on a characteristic time scale, $\tau_s \sim 6\pi\eta a^3/K = nk_B T a^2/KD$, with D being the particle diffusivity. Relaxations of force dipoles and of the configurational distribution of the attached polymer chains compete with strain propagation to determine the long-time behavior of the material. We conjecture that strong interparticle correlations in the nanoparticle fluids lead to long dipole lifetimes and allow for faster propagation of strain than dipole relaxation, which manifests as bulk hyperdiffusion.

Initial insights into the competition between the various relaxation processes can therefore be obtained by comparing the relevant time scales. The ratio of the diffusive relaxation time scale¹⁷ ($\tau_D \sim a^2/D$) and the strain propagation time scale, τ_s , are reported in Figure 3A. The ratio ($=K/nk_B T$) is seen to be consistently larger than unity, signifying that the strain generated by thermally induced fluctuations propagates at a

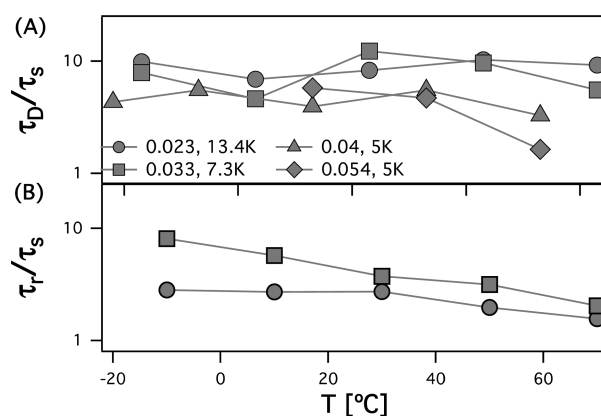


Figure 3. Ratios of (A) diffusive relaxation time scale τ_D and strain propagation time scale τ_s and (B) the characteristic relaxation time as probed by shear measurements τ_r and τ_s as a function of temperature T for various PI–SiO₂ nanoparticle fluids. The lines are guides to the eye.

faster rate than the rate at which diffusion relaxes the shear modes of the fluid. At the same time, the ratio of τ_r to τ_s ($=KD/nk_B T a^2 \dot{\gamma}_p$, Figure 3B) decreases with temperature, consistent with the idea that bulk relaxations arising from motions of the attached polymer chains become increasingly effective in competing with, and eventually overtaking, strain propagation as the temperature rises. These physics provide a straightforward explanation for the transition from force–dipole driven hyperdiffusive relaxation to diffusive relaxation observed at the lowest particle loadings ($\phi = 0.023$ and 0.033) and at the highest temperature, 70 °C when $\tau_r/\tau_s \sim 1$. While the condition $\tau_s < \tau_r$ provides an accurate criterion for hyperdiffusion in our materials, one should recall that hyperdiffusion also requires either non-Brownian dynamics or a nonequilibrium state of the volume modes as noted above. Two additional aspects of the estimates are noteworthy: (i) the τ_r/τ_s ratios are presented only for materials ($\phi = 0.023$ and 0.033) where an estimate of the particle diffusivity at all temperatures is possible by using the diffusivity values estimated from XPCS measurements and the Arrhenius equation for capturing the temperature dependence of the local diffusivity, and (ii) the comparisons are based on an estimate for the bulk modulus using the literature values of the Poisson ratio $\nu_p (=0.3)$ for homogeneous, isotropic materials and the formula, $K \sim 2(1 + \nu_p)/3(1 - 2\nu_p)\eta_0\dot{\gamma}_t = 2.17\eta_0\dot{\gamma}_t$.

More detailed insights into the origin of hyperdiffusive relaxations were pursued by extending the strain field relaxation (SFR) model proposed by Bouchaud and Pitard.³² We propose that the SFR framework can be used to treat force dipoles arising from correlated particles in our material. Estimates for the hyperdiffusion velocity can be obtained from eq 2, provided the magnitude of the thermal-fluctuation-induced force dipoles are known. Balancing the energy requirements, $nK(\Delta V)^2 = k_B T$, with ΔV being the change in the volume associated with the fluctuation in the interparticle distance, $\sim n^{-2/3}\Delta\lambda$, provided an estimate of the strength of the resultant force dipole $|\mathbf{P}_0|$ as

$$|\mathbf{P}_0| = \lambda \frac{\partial(nK(\Delta V)^2)}{\partial\lambda} = 2\lambda K \Delta\lambda n^{-1/3} = 2 \left(\frac{Kk_B T}{n} \right)^{1/2}$$

The hyperdiffusion velocity, v , was thus estimated³² as

$$v = (4/75^{2/3}) \sqrt{k_B T n^{1/3} N_c^{4/3} / K \theta^2} \quad (3)$$

Here, N_c represents the number of neighbors ($=12$). The average lifetime of a dipole θ in our single-component materials is related to the time scale required for rotational diffusion of a particle with reference to its neighbors. As a first approximation, we set the dipole collapse and macroscopic stress relaxation time τ_r to be equal because this could be expected to be the case for a material in which the dipoles are induced by the inherent thermal fluctuations in the orientation of the local microstructure.

The velocity estimates from expression 3 are expected to be most relevant in the slow collapse regime³² and are compared with the experimental hyperdiffusion velocity ($v = 1/\sqrt{q\tau}$) for the $\phi = 0.054$ material in Figure 4A. The agreement is good at all

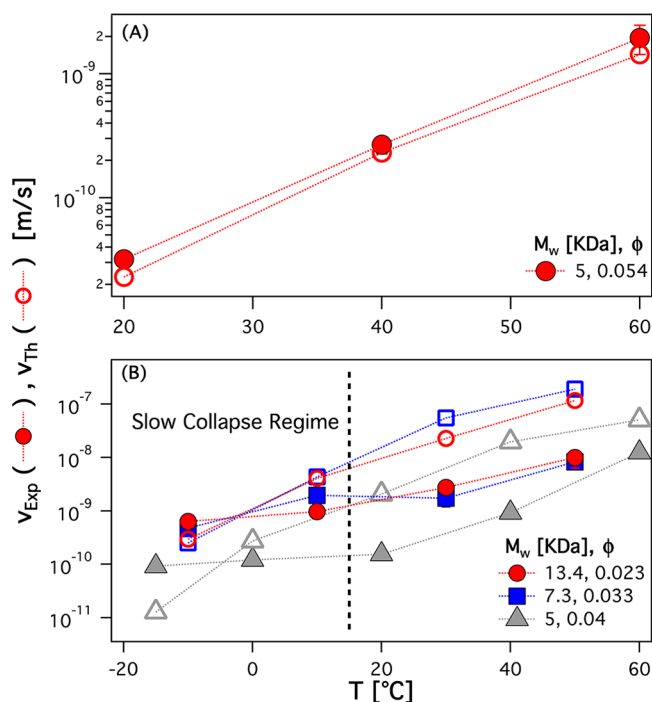


Figure 4. Experimental observations (filled symbols) and theoretical estimates (open symbols) of hyperdiffusion velocity v as a function of temperature T for (A) 5 kDa PI-SiO₂ ($\phi = 0.054$) and (B) 13.4 kDa PI-SiO₂ ($\phi = 0.023$), 7.3 kDa PI-SiO₂ ($\phi = 0.033$), and 5 kDa PI-SiO₂ ($\phi = 0.04$) nanoparticle fluids. The dashed vertical line in (B) denotes the transition between the $\tau_p/\tau_r \ll 1$ and the $\tau_p/\tau_r \sim 1$ regions.

temperatures studied, particularly considering the simplicity of the analysis and the crude estimates for K and θ used for the comparisons. Results shown in Figure 4B indicate that the extended Bouchaud–Pitard analysis is also able to provide rough estimates for other materials ($\phi \leq 0.04$), but only in the slow collapse regime (see SI for details). While we discount the surprisingly good agreement between the measured and calculated hyperdiffusion velocity owing to the simple theoretical analysis and the crude estimates for bulk modulus and dipole lifetime used in the calculations, the qualitatively similar behavior with temperature lends support to our hypothesis that strain fields arising in response to thermal fluctuations can produce hyperdiffusive relaxation in self-suspended materials.

We conclude the report with a more careful study of the role temperature plays in the relaxation dynamics in the higher ϕ fluids. Strong stretching and space filling constraints imposed

on polymer chains in self-suspended materials have previously been reported to produce increased particle correlations with increasing temperature.¹⁹ Figure 1D shows that for the fluid with $\phi = 0.033$, τ decreased with temperature T , as expected, whereas for a fluid with $\phi = 0.114$ (Figure S1E), there was an unexpected increase in τ with increasing T . These behaviors are more succinctly summarized in Figure 5, which reports the

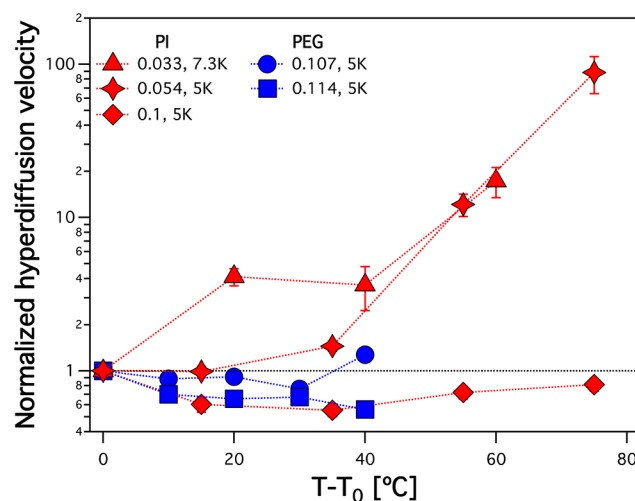


Figure 5. Normalized hyperdiffusion velocity vs adjusted temperature $T - T_0$ for 7.3 kDa PI-SiO₂ ($T_0 = -10$ °C), 5 kDa PI-SiO₂ ($T_0 = -15$ °C), and 5 kDa PEG-SiO₂ ($T_0 = 70$ °C) nanoparticle fluids. The lines are guide to the eye. Legend describes the ϕ and the tethered polymer M_w of the samples.

normalized hyperdiffusion velocity (v/v_{T_0}) in a variety of self-suspended fluids. Irrespective of the polymer attached to the nanoparticle core, v was seen to increase monotonically with T for low ϕ ($\phi \leq 0.054$); for intermediate ϕ ($\phi = 0.1, 0.107$), an initial decrease in v was followed by an upturn; for the most sparsely grafted particles ($\phi = 0.114$), v decreased monotonically with T . The unexpected decrease in v with T concurs with the previously reported thermal jamming¹⁹ in similar nanoparticle fluids and highlights the nontrivial role of temperature in soft materials.

Thus, with an increasing number of reports of hyperdiffusive dynamics in soft materials, the results presented here provide new insights about the origins of the phenomenon. The strongly correlated structure of the single-component nanoparticle fluids studied allows slowly relaxing particle dipoles, which are typically absent in glassy or jammed systems, to induce hyperdiffusive relaxations even in nanoparticle fluids that exhibit Newtonian flow properties and appear to be able to reach equilibrium in simple shear flow. The minimalistic material platform also allows for simple scaling arguments that tentatively describe the relaxations that produce hyperdiffusive dynamics using an extension of a generic theoretical approach.

■ ASSOCIATED CONTENT

Supporting Information

The Supporting Information is available free of charge on the ACS Publications website at DOI: 10.1021/acsmacrolett.5b00319.

Materials and methods, theoretical framework, and supporting Figures S1–S4 (PDF).

AUTHOR INFORMATION

Corresponding Author

*E-mail: laa25@cornell.edu.

Author Contributions

‡These authors contributed equally (S.S. and P.A.).

Notes

The authors declare the following competing financial interest(s): Prof. Archer is a Founder and Board Member of NOHMs Technologies, a technology start-up engaged in commercializing secondary batteries based on polymer–nanoparticle hybrid electrodes and electrolytes.

ACKNOWLEDGMENTS

This work was supported by the National Science Foundation Award No. DMR-1006323 and by Award No. KUS-C1018-02, made by King Abdullah University of Science and Technology (KAUST). Use of the Advanced Photon Source, operated by Argonne National Laboratory, was supported by the U.S. DOE under Contract No. DE-AC02-06CH11357.

REFERENCES

- (1) Cipelletti, L.; Manley, S.; Ball, R. C.; Weitz, D. A. *Phys. Rev. Lett.* **2000**, *84*, 2275.
- (2) Ramos, L.; Cipelletti, L. *Phys. Rev. Lett.* **2001**, *87*, 245503.
- (3) Cipelletti, L.; Ramos, L.; Manley, S.; Pitard, E.; Weitz, D. A.; Pashkovski, E. E.; Johansson, M. *Faraday Discuss.* **2003**, *123*, 237.
- (4) Bandyopadhyay, R.; Liang, D.; Yardimci, H.; Sessoms, D. A.; Borthwick, M. A.; Mochrie, S. G. J.; Harden, J. L.; Leheny, R. L. *Phys. Rev. Lett.* **2004**, *93*, 228302.
- (5) Cipelletti, L.; Ramos, L. *J. Phys.: Condens. Matter* **2005**, *17*, R253.
- (6) Narayanan, R.; Thiyagarajan, P.; Lewis, S.; Bansal, A.; Schadler, L.; Lurio, L. *Phys. Rev. Lett.* **2006**, *97*, 075505.
- (7) Guo, H.; Wilking, J.; Liang, D.; Mason, T.; Harden, J.; Leheny, R. *Phys. Rev. E* **2007**, *75*, 041401.
- (8) Guo, H.; Bourret, G.; Corbierre, M.; Rucareanu, S.; Lennox, R.; Laaziri, K.; Piche, L.; Sutton, M.; Harden, J.; Leheny, R. *Phys. Rev. Lett.* **2009**, *102*, 075702.
- (9) Mazoyer, S.; Cipelletti, L.; Ramos, L. *Phys. Rev. E* **2009**, *79*, 011501.
- (10) Madsen, A.; Leheny, R. L.; Guo, H.; Sprung, M.; Czakkel, O. *New J. Phys.* **2010**, *12*, 055001.
- (11) Lieleg, O.; Kayser, J.; Brambilla, G.; Cipelletti, L.; Bausch, A. R. *Nat. Mater.* **2011**, *10*, 236.
- (12) Kim, D.; Srivastava, S.; Narayanan, S.; Archer, L. A. *Soft Matter* **2012**, *8*, 10813.
- (13) Srivastava, S.; Archer, L. A.; Narayanan, S. *Phys. Rev. Lett.* **2013**, *110*, 148302.
- (14) Kwaśniewski, P.; Madsen, A.; Fluerasu, A. *Soft Matter* **2014**, *10*, 8698.
- (15) Tamborini, E.; Cipelletti, L.; Ramos, L. *Phys. Rev. Lett.* **2014**, *113*, 078301.
- (16) Ruta, B.; Chushkin, Y.; Monaco, G.; Cipelletti, L.; Pineda, E.; Bruna, P.; Giordano, V. M.; Gonzalez-Silveira, M. *Phys. Rev. Lett.* **2012**, *109*, 165701.
- (17) Russel, W. B.; Saville, D. A.; Schowalter, W. R. In *Colloidal Dispersions*; Batchelor, G. K., Ed.; Cambridge University Press: New York, 1992.
- (18) Agarwal, P.; Qi, H.; Archer, L. A. *Nano Lett.* **2010**, *10*, 111.
- (19) Agarwal, P.; Srivastava, S.; Archer, L. A. *Phys. Rev. Lett.* **2011**, *107*, 268302.
- (20) Agarwal, P.; Kim, S. A.; Archer, L. A. *Phys. Rev. Lett.* **2012**, *109*, 258301. Kim, S. A.; Mangal, R.; Archer, L. A. *Macromolecules* **2015**, *48*, 6280.
- (21) Akcora, P.; Liu, H.; Kumar, S. K.; Moll, J.; Li, Y.; Benicewicz, B. C.; Schadler, L. S.; Acehan, D.; Panagiotopoulos, A. Z.; Pryamitsyn, V.;

Ganesan, V.; Ilavsky, J.; Thiyagarajan, P.; Colby, R. H.; Douglas, J. F. *Nat. Mater.* **2009**, *8*, 354.

(22) Srivastava, S.; Agarwal, P.; Archer, L. A. *Langmuir* **2012**, *28*, 6276.

(23) Kumar, S. K.; Jouault, N.; Benicewicz, B.; Neely, T. *Macromolecules* **2013**, *46*, 3199.

(24) Mazoyer, S.; Cipelletti, L.; Ramos, L. *Phys. Rev. Lett.* **2006**, *97*, 238301.

(25) Duri, A.; Cipelletti, L. *Europhys. Lett.* **2006**, *76*, 972.

(26) Robert, A.; Wandersman, E.; Dubois, E.; Dupuis, V.; Perzynski, R. *Europhys. Lett.* **2006**, *75*, 764.

(27) Caronna, C.; Chushkin, Y.; Madsen, A.; Cupane, A. *Phys. Rev. Lett.* **2008**, *100*, 055702.

(28) Falus, P.; Borthwick, M. A.; Narayanan, S.; Sandy, A. R.; Mochrie, S. G. J. *Phys. Rev. Lett.* **2006**, *97*, 066102.

(29) Franosch, T.; Götze, W. *J. Phys. Chem. B* **1999**, *103*, 4011.

(30) Yu, H. Y.; Koch, D. L. *Langmuir* **2010**, *26*, 16801.

(31) Yu, H.-Y.; Srivastava, S.; Archer, L. A.; Koch, D. L. *Soft Matter* **2014**, *10*, 9120.

(32) Bouchaud, J. P.; Pitard, E. *Eur. Phys. J. E: Soft Matter Biol. Phys.* **2002**, *9*, 287.